TÜBİTAK

Turkish Journal of Biology

http://journals.tubitak.gov.tr/biology/

Research Article

Turk J Biol
(2017) 41: 835-842
© TÜBİTAK
doi:10.3906/biy-1705-37

Effect of mutation in active site residue Trp209 to Val, Leu, Ile and Pro on the catalytic activity and affinity for some benzenesulfonamides of human carbonic anhydrase II

Deryanur KILIÇ[1,2], Orhan ERDOĞAN[3], Ömer İrfan KÜFREVİOĞLU[1,*]

[1]Department of Chemistry, Faculty of Science, Atatürk University, Erzurum, Turkey
[2]Department of Chemistry, Faculty of Science and Letters, Aksaray University, Aksaray, Turkey
[3]Department of Molecular Biology and Genetics, Faculty of Science, Atatürk University, Erzurum, Turkey

Received: 11.05.2017 • **Accepted/Published Online:** 13.08.2017 • **Final Version:** 10.11.2017

Abstract: Human carbonic anhydrase II (hCA II) enzyme was firstly expressed using a pET-SUMO expression vector in *Escherichia coli* and the recombinant enzyme was purified using nickel (Ni^{2+}) affinity chromatography. The substitutions of Trp 209 with four amino acid (Val, Leu, Ile, and Pro) in the hydrophobic pocket of hCA II were conducted using site-directed mutagenesis. The p-nitrophenyl esterase activity of hCA II variants correlates with the hydrophobicity and size of residue, suggesting that the hydrophobic character of this residue is important for catalysis. The Trp 209 was forecast as an important residue and was exposed to computational mutagenesis. This forecast was confirmed experimentally by producing hCA II mutants and determining the resulting affinities towards some benzenesulfonamides. These mutations in the hydrophobic pocket of the enzyme active site decreased the protein expression of hCA II in *E. coli*, causing the formation of insoluble protein aggregates in many cases. Our findings demonstrated that the Trp 209 in hCA II plays an important role in the folding process and the valine residues are very compatible for the hydrophobic region in the active cavity of this isoenzyme. These mutant proteins will lead to a better understanding of structural functions and drug-based studies in the future.

Key words: Computational mutagenesis, enzyme inhibitor, human carbonic anhydrase II, site-directed mutagenesis, sulfonamide

1. Introduction

Carbonic anhydrase (CA, EC 4.2.1.1) is in the metalloenzyme family and catalyzes the reversible hydration of CO_2 through two steps, as shown in the following reaction: (i) the formation of HCO_3^- resulting from a nucleophilic attack by a Zn–OH^- on CO_2. (ii) Transfer of H^+ from the Zn–H_2O to Zn–OH^- for catalysis of the next reaction (Silverman and Lindskog, 1988; Ekinci et al., 2011; Senturk et al., 2011).

$$\text{(i)}\ E:Zn-OH^- + CO_2 \xrightleftharpoons{H_2O} E:Zn-H_2O + HCO_3^-$$

$$\text{(ii)}\ E:Zn-H_2O + B \rightleftharpoons E:Zn\text{-}OH^- + BH^+$$

(B: H^+ acceptor of solvent)

The human CA (hCA) family involves sixteen different α-isoforms. Five of them are cytosolic, two different forms of CA V are mitochondrial, one is secreted in saliva, and the others are membrane-bound isoforms (Supuran and Scozzafava, 2007; Supuran, 2008).

The active site of mammalian CAs is split into two parts as hydrophobic and hydrophilic. The hydrophobic and hydrophilic parts include residues in position 121, 131, 141, 143, 198, and 209 and in position 62, 64, 67, 92, and 200 (Fierke et al., 1991; Elleby et al., 1999; Fisher et al., 2007; Domsic et al., 2008; Mikulski et al., 2011a, 2011b). Many mutation studies have been done in the hydrophobic pocket, where the substrate binds (Fierke et al., 1991; Hunt and Fierke, 1997; Elleby et al., 1999). Therefore, we decided to carry out the mutation of Trp209 residue in the hydrophobic part of the enzyme active site cavity. In this study, the mutants of Trp209 caused modifications of the steric volume in the cavity and then were investigated how these changes affected the binding some benzenesulfonamide inhibitors to the active site and the catalytic activity of hCA II.

We have noted the catalytic properties of four different mutant enzymes (Trp209Ile, Trp209Leu, Trp209Val, and Trp209Pro) and the affinity of some benzenesulfonamides on these mutant enzymes.

* Correspondence: okufrevi@atauni.edu.tr

2. Materials and methods

2.1. Bacterial strains and reagents

Champion pET SUMO Expression System, *E. coli* One Shot Mach1-T1^R, *E. coli* BL21 (DE3) One Shot, ProBond Ni-NTA resin, adult human pancreas cDNA, pET-SUMO vector, and SUMO protease were purchased from Invitrogen (USA). QuikChange II Site-Directed Mutagenesis Kit and XL10-Gold ultra-competent cells were obtained from Stratagene. All other analytical grade chemicals were obtained from Sigma (Germany).

2.2. Cloning of hCA II enzymes and site-directed mutagenesis

The coding sequence of hCA II (GenBank accession number NM_000067.2) was amplified by PCR using the forward primer 5'-ATGTCCCATCACTGGGGGTA-3' and the reverse primer 5'-TTATTTGAAGGAAGCTTTGA TTTGCCTGTT-3'. The PCR process was performed as follows: 4 min at 94 °C, 35 cycles of 1 min at 94 °C, 1 min at 60 °C, and 1 min at 72 °C, followed by 10 min at 72 °C. The PCR product was directly ligated into the linear pET-SUMO vector with 1:1 molar ratio using T4 DNA ligase overnight at 16 °C according to the manufacturer's instructions (Champion pET SUMO protein expression system kit). Then the ligated product was transformed into One Shot Mach1-T1^R competent *E. coli* cells. Positive colonies were chosen from a Luria-Bertani (LB) agar plate including kanamycin (50 µg/mL). Plasmids were obtained from the positive colony by using the Plasmid Miniprep kit. SUMO forward primer and T7 reverse primer were used to verify DNA sequencing.

Site-directed mutagenesis was performed on the pET-SUMO-hCA II according to the protocol of the QuikChange Site-Directed Mutagenesis Kit. The mutant primers obtained from Methabion as shown in Table 1 were used to perform the site-directed mutagenesis based on PCR. The PCR reaction mixture was prepared by adding 10X reaction buffer, template (90 ng), primers (125 ng), dNTP mix, Quik Solution reagent, ddH_2O, and finally QuikChange Lightning Enzyme. The pET-SUMO-hCA II was amplified as follows: 2 min at 95 °C (first denaturation step), 18 cycles of 20 s at 95 °C (denaturation), 10 s at 68 °C (annealing), and 3 min at 68 °C (extension), followed by 5 min at 68 °C (last denaturation step). The amplified product was digested with *DpnI* and transformed into XL10-Gold ultra-competent cells. The MedSanTek Company (Turkey) performed the sequence analysis to define sequences of the entire coding region.

2.3. Expression and purification of the wild-type and mutant hCA IIs

Pilot expression of the wt and mutant hCA IIs was carried out by inducing with isopropyl-1-thio-β-D-galactopyrasonide (IPTG). Briefly, an overnight culture (500 µL) was added to 10 mL of LB broth including kanamycin (50 µg/mL) and then incubated at 37 °C for 2 h by shaking to mid-log phase ($O.D._{600}$~0.4–0.6). Until the final concentration was 1 mM, IPTG was added to the culture and 500 µL of culture was centrifuged at intervals of an hour (0–6 h) at 10,000 × *g* for 30 s. The cell pellets were stored at –20 °C. To determine whether the protein was expressed, SDS-PAGE analysis of each pellet was carried out.

Recombinant plasmids of the wt and mutant were transformed into the *E. coli* strain BL21 (DE3) for expression. The cells covering the recombinant proteins were grown in LB broth with kanamycin (50 µg/mL). IPTG (1 mM) was added to the culture with optic density of 0.5 and this culture was incubated at 37 °C for 6 h. To disrupt harvested cells, pellets were sonicated, frozen, and thawed, in that order. The proteins were purified using a ProBond Ni-NTA resin according to the instructions of the manufacturer. NaH_2PO_4 buffer (pH 8.0), imidazole (250 mM), and NaCl (0.5 M) were used to elute the pure

Table 1. Designed primers for site-directed mutagenesis.

Primer	Sequence (5'-3')
W209I For	5'-GATGGGTTCCTTGAGCACAATTATGGTCACACATTCCAGAAGAGG-3
W209I Rev	5'-CCTCTTCTGGAATGTGTGACCATAATTGTGCTCAAGGAACCCATC-3'
W209L For	5'-GTTCCTTGAGCACAATCAAGGTCACACATTCCAGA-3'
W209L Rev	5'-TCTGGAATGTGTGACCTTGATTGTGCTCAAGGAAC-3'
W209P For	5'-GGTTCCTTGAGCACAATCGGGGTCACACATTCCAGAAG-3'
W209P Rev	5'-CTTCTGGAATGTGTGACCCCGATTGTGCTCAAGGAACC-3'
W209V For	5'-GGGTTCCTTGAGCACAATCACGGTCACACATTCCAGAAGA-3'
W209V Rev	5'-TCTTCTGGAATGTGTGACCGTGATTGTGCTCAAGGAACCC-3'

proteins. The purity and molecular weight of the purified SUMO-hCA II was determined by SDS-PAGE analysis (Supplementary file in Figure S1), using Coomassie blue staining. The buffer in fractions of the SUMO-hCA II and mutants was exchanged with Tris-HCl buffer (20 mM pH 8.0, 150 mM NaCl) to digest with SUMO protease and then concentrated up to 1.5–2 mL using an Amicon filter. To disrupt the fusion proteins, the mixture was incubated with SUMO protease at 30 °C for 2–3 h. The digested protein was verified by SDS-PAGE analysis (Supplementary file in Figure S2).

2.4. hCA II inhibition experiments

The hCA II activity was measured at 348 nm spectrophotometrically during the conversion of 4-nitrophenylacetate to 4-nitrophenylate according to Verpoorte et al. (1967). Inhibition effects of the compounds (3,4-diamino-benzenesulfonamide **1**, 3-amino-4-chlorobenzenesulfonamide **2**, 5-amino-2-methylbenzenesulfonamide **3**, and acetazolamide **4**) on SUMO fusion the wt and mutant enzymes were analyzed in their different concentrations. The Cheng–Prusoff equation was used to determine the K_i values of each compound (Scott et al., 2009).

2.5. Computational site-directed mutagenesis

The protein crystal structure of hCA II (PDB ID: 2WEJ) was obtained using the RCSB Protein Data Bank (Maestro, version 10.5, Schrodinger, LLC; 2015). The Protein Preparation Wizard (Schrödinger) was used to organize the protein structures (Sastry et al., 2013). This wizard assigned bond order and formal charges, incorporated hydrogens, constructed side chains and loops with missing atoms, defined the ideal protonation conditions for ionizable residues, and made a restrained minimization.

Computational mutagenesis was performed using Maestro, version 10.5, Schrodinger. The Trp209Val, Trp209Leu, Trp209Ile, and Trp209Pro single-point mutations were generated using the Residue Scanning module of BioLuminate and their interactions with nearby residues were represented using a 2D ligand interaction diagram (Figure 1). After the mutagenesis, each protein was optimized and minimized by OPLS_2005 force field in the wizard. After energy minimization, the important residues in active site of the mutant structures were superimposed with the corresponding native structure (Figure 2).

3. Results

The hydrophobic part (Val 121, Val 143, Leu 198, and Trp 209) in the active site of hCA II is related to both substrate/inhibitor binding and the catalyst of the CO_2 hydration (Alexander et al., 1991; Domsic et al., 2008; West et al., 2012).

Both experimental and computational analyses were performed to understand the functional significance in the hydrophobic package and to clarify the catalytic function of Trp 209 in the active site of hCA II. The combination of the analyses with the mutants obtained in various size and hydrophobicity helps us to understand the mechanisms of this residue in the catalytic process well. Therefore, we exchanged the Trp209 with four hydrophobic residues (Trp209Ile, Trp209Leu, Trp209Val, and Trp209Pro) experimentally. In addition, computational mutagenesis of the Trp209 was performed using Maestro, version 10.5. The results of the computational mutagenesis are presented in Table 2; bonds and positions of the mutated residues and the Trp209 are shown in the 2D ligand interaction diagram of Maestro (Figure 1). Active site residues and ligand (benzenesulfonamides) of mutants in the hCA II structure (PDB: 2WEJ) were superimposed with the corresponding native structure (Figure 2).

K_M and k_{cat} values of hCA II the wt and mutants (Trp209Leu, Trp209Ile, Trp209Val, and Trp209Pro) were determined and are presented in Table 3. In addition to kinetic properties, the affinity for some benzenesulfonamides was examined for the wt and mutant enzymes. When compared to the wt, compounds **1–4** showed dramatically reduced affinity for the four mutants (Table 4). The data of the sequence results were aligned to confirm the mutations experimentally performed at position 209 of hCA II (Figure 3).

4. Discussion

Mutants of CA I and CA II have been obtained and enzyme activities of these mutants have been associated with wild-type in many studies. CO_2 and 4-nitrophenylacetate were used as a substrate in these enzyme assays (Nair et al., 1991; Nair and Christianson, 1993; Fisher et al., 2005; Jiang et al., 2008; Kockar et al., 2010; Mikulski et al., 2011a, 2011b; Wu et al., 2011; Fisher et al., 2012; Turkoglu et al., 2012; Halder and Taraphder, 2013). The earlier work confirmed that specific substitutes of residue in the hydrophobic pocket were related to variations in catalytic rates of hCA II (Fierke et al., 1991; Krebs et al., 1993; Host and Jonsson, 2008). While the exchanges of Asn67 to Ile, Gln92 to Val, and Leu204 to Ser in the active site of hCA II were carried out by Turkoglu et al. (2012), W209I, W209L, W209V, and W209P mutant enzymes were obtained in our study. The mutations at Val 143 at the CO_2 binding site of hCA II lead to important modifications in the three-dimensional protein structure and catalytic activity (Fierke et al., 1991). In other research, the spectral effects of tryptophan residues were studied by substituting the tryptophan residues in hCA II (W5F, W16F, W97C, W123C, W192F, W209F, and W245C) and also W209G and W209S, which conserved the hydrophobic face in hCAII, were

Table 2. Residue scanning results of wild-type and mutants of hCA II enzymes.

Protein	Mutations	Solvent Accessible Area (nm/S2/N)			Δ Stability (Solvated) kcal/mol	Δ Stability (Covalent) kcal/mol
		Total	Hydrophobic	Hydrophilic		
hCA II	W209P	25.7	12.03	12.32	50.07	26.79
	W209I	7.99	3.72	3.98	11.35	12.18
	W209L	1.67	0.86	0.79	6.84	4.37
	W209V	15.56	7.33	7.66	12.81	2.17

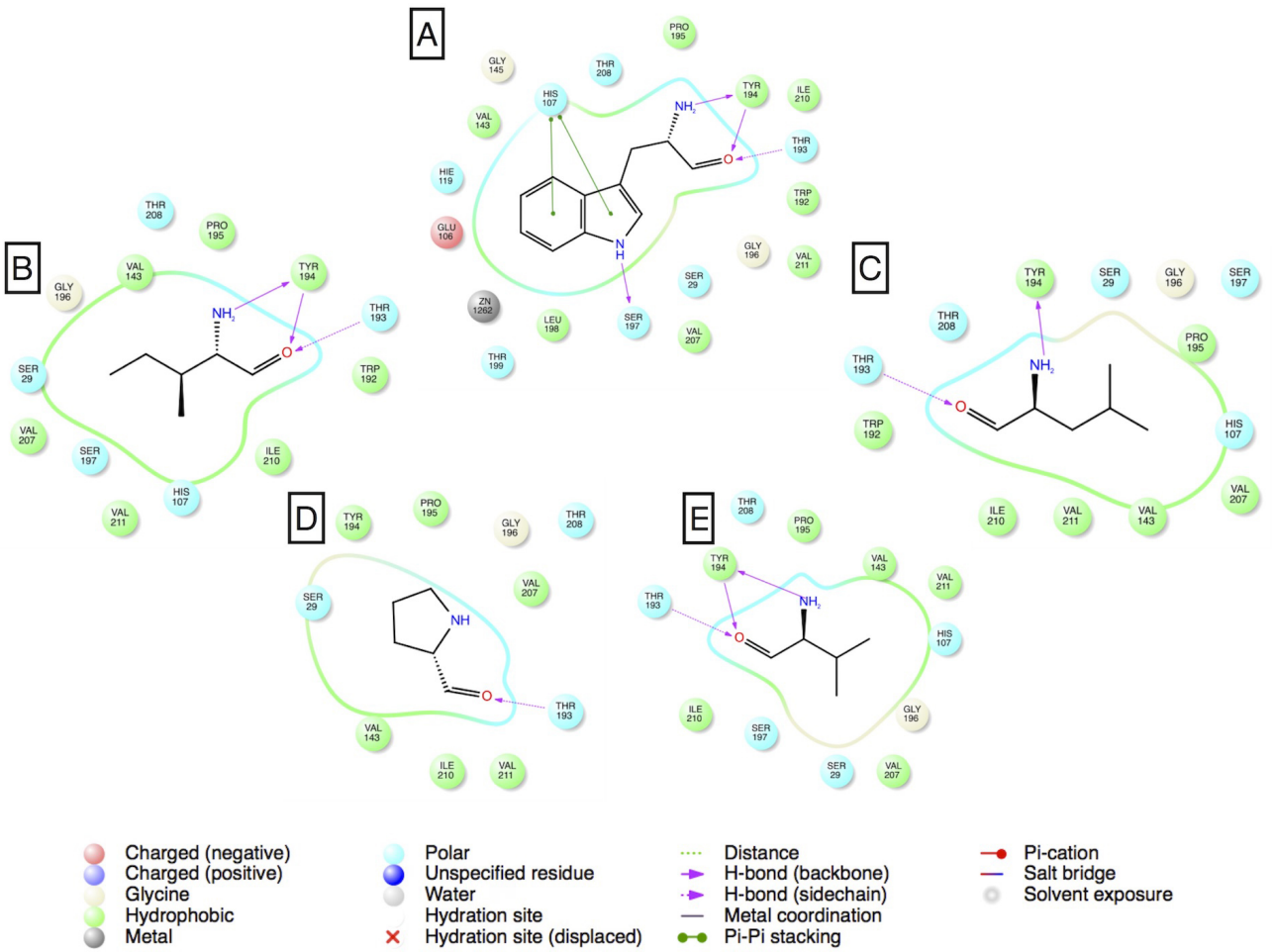

Figure 1. Molecular interactions along with nearby residues of W209 (A), W209I (B), W209L (C), W209P (D), W209V (E) are represented in 2D diagrams. Pink arrows symbolize a hydrogen bond interaction with a protein backbone atom (solid line) and a protein side chain (dashed line). Two-point green line represents π–π stacking.

investigated by mutagenesis (Krebs and Fierke, 1993; Freskgard et al., 1994).

The mutants of Trp 209 in hCA II assessed in this study made modifications in the steric volume of the active-site cavity. The replacement of Trp209 in wild-type (side-chain volume 229 Å^3) by Ile (167 Å^3), Leu (167 Å^3), Val (140 Å^3), and Pro (113 Å^3) exhibited the effect of reduced steric volume of the active-site cavity. The reduced volume in the active-site cavity of W209I, W209L, W209V, and W209P mutant enzymes triggered the fall in catalytic activity. The W209V mutant showed similar specific activity compared to the wt enzyme, while the W209P, W209L,

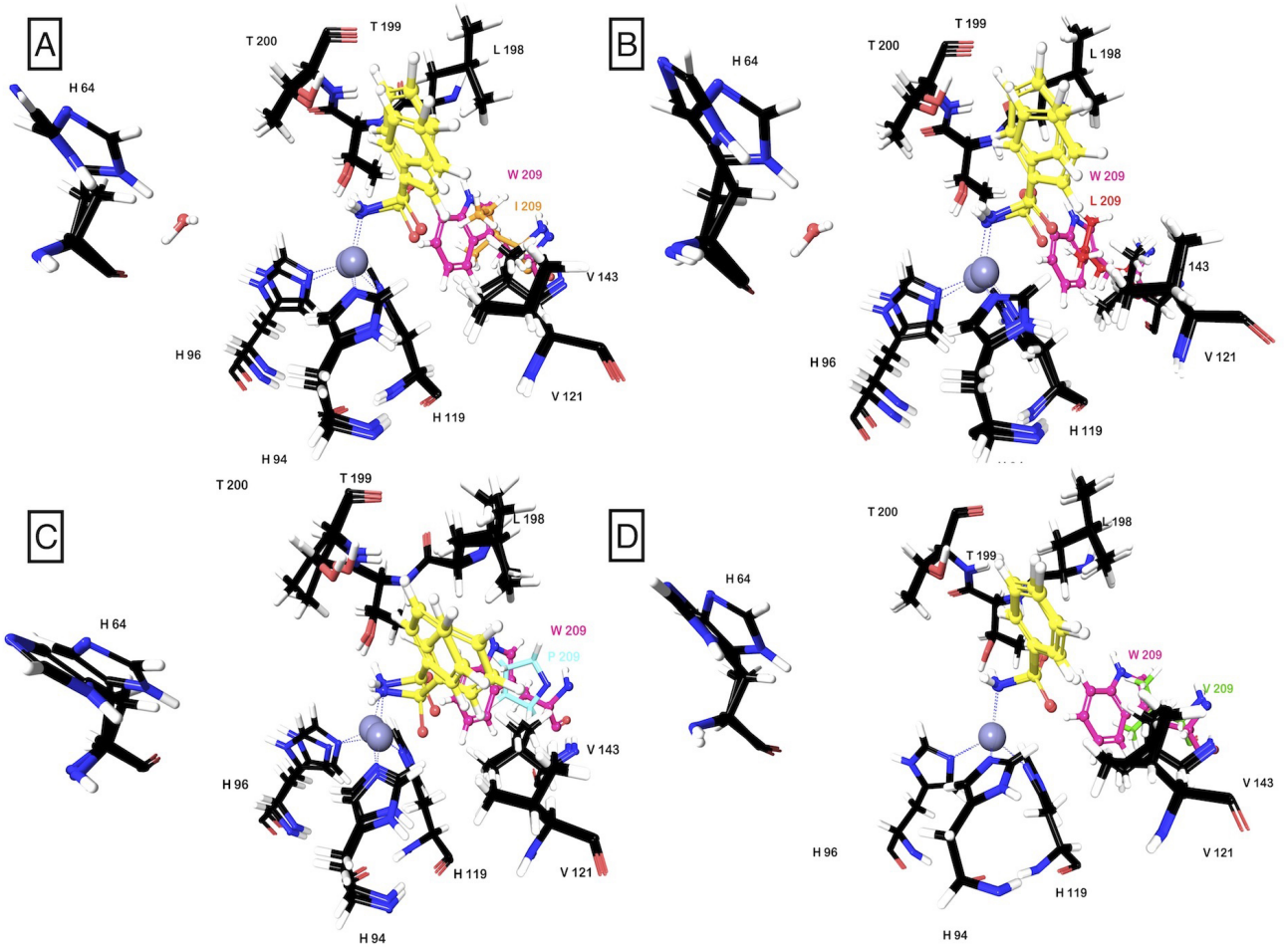

Figure 2. The important residues in active sites of W209I (A), W209L (B), W209P (C), and W209V (D) are superimposed with that of wild-type. In all superimpose images, W209 is represented in a ball and stick model with salmon pink carbon atoms and white hydrogen atoms, benzenesulfonamide is represented in a ball and stick model with yellow carbon atoms and blue nitrogen atoms, important residues (H64, H94, H96, H119, V143, V121, L198, T199 and T200) are represented in a thin tube model with black carbon and red oxygen atoms, Zn atoms are represented as gray balls, and I209, L209, P209, and V209 in the mutant structure are represented in a ball and stick model with orange, red, turquoise, and green carbon atoms, respectively.

Table 3. The K_M and kcat values of wild-type and mutants of hCA II enzymes (Trp209Leu, Trp209Ile, Trp209Val, and Trp209Pro).

Isoenzymes	Protein details	K_M (mM)	k_{cat} (s^{-1})
hCA II	wt	1.61 ± 0.07	3.30 ± 0.19
hCA II	Trp209Leu	0.75 ± 0.12	1.81 ± 0.11
hCA II	Trp209Ile	0.51 ± 0.06	0.90 ± 0.81
hCA II	Trp209Pro	1.02 ± 0.07	0.35 ± 0.14
hCA II	Trp209Val	0.74 ± 0.07	2.80 ± 0.09

[a] The data performed in triplicate (mean ± SD)

Table 4. Inhibition of the wild-type and mutants with the compounds **1**–**4**, by an esterase assay.

Compounds	K_i (μM)				
	hCA II	Trp209Pro	Trp209Leu	Trp209Ile	Trp209Val
1	2.03 ± 0.12	969 ± 17	734 ± 6	671 ± 10	541 ± 9
2	9.05 ± 0.11	1209 ± 23	635 ± 6	540 ± 4	242 ± 6
3	2.80 ± 0.02	252 ± 7	125 ± 5	131 ± 7	121 ± 5
4 (AZA)	0.052 ± 0.004	125 ± 4	40.8 ± 3.1	30.3 ± 1.8	8.2 ± 0.8

[a] The data performed in triplicate (mean ± SD)

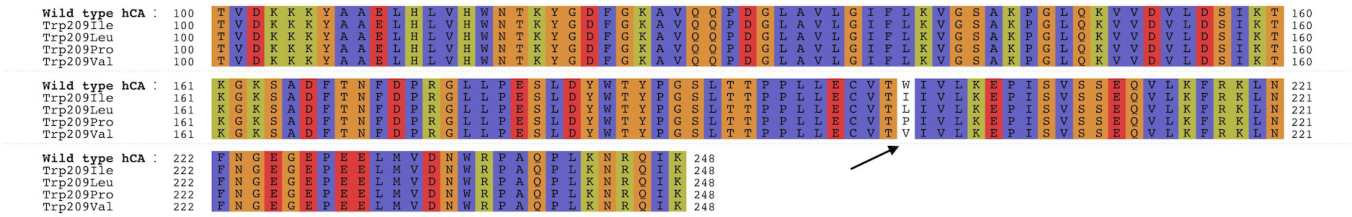

Figure 3. The sequences of hCA II wild-type and four mutants (Orange arrow represents wt, W209I, W209L, W209P, and W209V.

and W209I mutants were around 60%, 30%, and 20% less active for p-nitrophenyl esterase activity compared to the wt enzyme, respectively. The highest decrease in specific activity among the mutants was observed in Trp209Pro when compared to the wt. This result indicated the lacking a hydrophobic pocket could dramatically reduce the catalytic activity of hCA II.

Although the replacements do not affect to pathway of the H^+ transfer of this enzyme, there were changes in the rate constant (k_{cat}) that comprise assistance of H^+ transfer between the solvent and the active site. As seen in Table 3, the k_{cat} values for W209L, W209I, and W209P mutants were reduced by 2-, 3-, and 10-fold, compared with the wt, respectively, whereas the W209V mutant was very similar to the wt. The k_{cat} for a proton transfer from His64 to Zn–OH^- during catalysis was 3.30 s^{-1} for the wt. The W209V mutant was the fastest isoenzyme, with a value of 2.80 s^{-1}. The reduction in catalytic rate could be due to the increase in the active site cavity of the hCA II mutants.

Probably because the distance between substrate and Zn–OH^- is greater in the mutants, the contact formed with unpaired electrons of the oxygen atom of Zn–OH^- is reduced. The data in Table 3 show that the k_{cat} and K_M values of mutant enzymes were different from those of the wt. The K_M decreased considerably from 1.61 mM for the wt to 0.51 for the Trp209Ile. Inhibitory effects of the compounds, a small library of **3** sulfonamides and **1** acetazolamide, against the wt and mutant enzymes were investigated and it was also determined how they affect the inhibitor property (Table 4). The compounds **1**–**3** are simple aromatic/heterocyclic derivatives largely investigated by means of structural and inhibition studies, whereas acetazolamide **4** is a clinically used antiglaucoma drug. Recently, inhibition studies of CA isoenzymes have gained considerable attention for medicinal application (Senturk et al., 2011; Mete et al., 2016). It has been reported that the benzenesulfonamide derivatives commonly used in the inhibition of CAs have a potent inhibitory effect on hCA II (Casini et al., 2000; Cecchi et al., 2004; Innocenti et al., 2004; Alp et al., 2012; Mete et al., 2016; Yaseen et al., 2016).

When inhibition constants of the compounds **1**–**4** were compared, it was observed that mutants had dramatically higher values than the wt hCA II. These results showed that the compounds were less effective in the mutants. The K_i values of derivatives **1**–**4** were 125–1209 μM for the Trp209Pro mutant, 40.8–734 μM for the Trp209Leu mutant, 30.3–671 μM for the Trp209Ile mutant, and 8.2–541 μM for the Trp209Val mutant (Table 4). Our results showed that the highest decrease in the inhibition effect of this compounds on the enzyme was observed in the Trp209Pro mutant compared to the wt, followed by the Trp209Leu and Trp209Ile, while the smallest decrease in the inhibition effect was detected in the Trp209Val (except for compounds 3). These values suggested that the Trp209 residue change in the active site may cause significant irregularities in chemical bond interactions.

The changes in residue hydrophobicity were evaluated using the solvent-accessible surface area (SASA) stated by a water probe radius of 1.4 Å. The changes in total surface area (Δ SASA total) and in surface area of polar atoms (Δ SASA polar) and nonpolar atoms (Δ SASA nonpolar) due to the mutation were determined using BioLuminate, Schrödinger [16]. Additionally, the changes in the stability of the protein owing to the mutation were calculated using the prime energy function with an implicit solvent term (Table 2). When compared to the wt, these mutants exhibited the largest change in surface area in the Trp209Pro, followed by the Trp209Val, Trp209Ile, and Trp209Leu, whereas the change in covalent stability of the protein due to the mutation was least in the Trp209Val. This result showed that the changes in the covalent stability of the protein were parallel with the changes in enzyme activity. When superimposed structures were examined, it was observed that Zn metals and residues (His 94, His 96, and His 119) of wt and Trp209Val overlap in similar coordinates but not the others. As a result, Figure 2 shows that protein backbones of the Trp209Val and wt had very similar structures.

The amino acid residue (Trp 209) involved in the binding of substrate in the active site of the enzyme having physiological importance and being abundant was altered to residues with varying hydrophobicity and size. The W209V mutant showed similar specific activity values to the wt, whereas the W209P, W209L, and W209I mutants were less active around 60%, 30%, and 20% in esterase assay compared to the wt, respectively. The affinity of some benzenesulfonamides was also investigated for the mutant enzymes. When compared to the wt, compounds **1**–**4** showed dramatically reduced affinity for the four mutants. These data highlighted the function of the Trp 209 amongst the amino acids on the hydrophobic part of the active site in effective catalysis by hCA II. Surprisingly, the Trp209Val had better catalytic properties among the mutants and showed higher affinity for benzene sulfonamide inhibitors. As we know, the hydrophobic pocket of hCA II enzyme has valine residues (Val 121, Val 143) more than one. Thus, we concluded that the valine residue is compatible for the hydrophobic region of activity site of this isoenzyme. Moreover, our study showed that both the catalytic rate constants and the specific activity rates are related to the results of computational mutagenesis.

Acknowledgments

This study was financed by Atatürk University Scientific Research Council (Project No: Erzurum BAP-2012/155) and ÖYP (Faculty Development Program) of Atatürk University.

References

Alexander RS, Nair SK, Christianson DW (1991). Engineering the hydrophobic pocket of carbonic anhydrase-II. Biochemistry 30: 11064-11072.

Alp C, Ozsoy S, Alp NA, Erdem D, Gultekin MS, Kufrevioglu OI, Senturk M, Supuran CT (2012). Sulfapyridine-like benzenesulfonamide derivatives as inhibitors of carbonic anhydrase isoenzymes I, II and VI. J Enzym Inhib Med Ch 27: 818-824.

Casini A, Scozzafava A, Mincione F, Menabuoni L, Ilies MA, Supuran CT (2000). Carbonic anhydrase inhibitors: water-soluble 4-sulfamoylphenylthioureas as topical intraocular pressure-lowering agents with long-lasting effects. J Med Chem 43: 4884-4892.

Cecchi A, Winum JY, Innocenti A, Vullo D, Montero JL, Scozzafava A, Supuran CT (2004). Carbonic anhydrase inhibitors: synthesis and inhibition of cytosolic/tumor-associated carbonic anhydrase isozymes I, II, and IX with sulfonamides derived from 4-isothiocyanato-benzolamide. Bioorg Med Chem Lett 14: 5775-5780.

Domsic JF, Avvaru BS, Kim CU, Gruner SM, Agbandje-McKenna M, Silverman DN, McKenna R (2008). Entrapment of carbon dioxide in the active site of carbonic anhydrase II. J Biol Chem 283: 30766-30771.

Ekinci D, Ceyhun SB, Senturk M, Erdem D, Kufrevioglu OI, Supuran CT (2011). Characterization and anions inhibition studies of an alpha-carbonic anhydrase from the teleost fish *Dicentrarchus labrax*. Bioorgan Med Chem 19: 744-748.

Elleby B, Sjoblom B, Lindskog S (1999). Changing the efficiency and specificity of the esterase activity of human carbonic anhydrase II by site-specific mutagenesis. Eur J Biochem 262: 516-521.

Fierke CA, Calderone TL, Krebs JF (1991). Functional consequences of engineering the hydrophobic pocket of carbonic anhydrase II. Biochemistry 30: 11054-11063.

Fisher SZ, Tu C, Bhatt D, Govindasamy L, Agbandje-McKenna M, McKenna R, Silverman DN (2007). Speeding up proton transfer in a fast enzyme: kinetic and crystallographic studies on the effect of hydrophobic amino acid substitutions in the active site of human carbonic anhydrase II. Biochemistry 46: 3803-3813.

Fisher Z, Boone CD, Biswas SM, Venkatakrishnan B, Aggarwal M, Tu C, Agbandje-McKenna M, Silverman D, McKenna R (2012). Kinetic and structural characterization of thermostabilized mutants of human carbonic anhydrase II. Protein Eng Des Sel 25: 347-355.

Fisher Z, Prada JAH, Tu C, Duda D, Yoshioka C, An HQ, Govindasamy L, Silverman DN, McKenna R (2005). Structural and kinetic characterization of active-site histidine as a proton shuttle in catalysis by human carbonic anhydrase II. Biochemistry 44: 1097-1105.

Freskgard PO, Martensson LG, Jonasson P, Jonsson BH, Carlsson U (1994). Assignment of the contribution of the tryptophan residues to the circular-dichroism spectrum of human carbonic-anhydrase II. Biochemistry 33: 14281-14288.

Halder P, Taraphder S (2013). Modeling the structure and proton transfer pathways of the mutant His-107-Tyr of human carbonic anhydrase II. J Mol Model 19: 289-298.

Host GE, Jonsson BH (2008). Converting human carbonic anhydrase II into a benzoate ester hydrolase through rational redesign. Bba-Proteins Proteom 1784: 811-815.

Hunt JA, Fierke CA (1997). Selection of carbonic anhydrase variants displayed on phage - aromatic residues in zinc binding site enhance metal affinity and equilibration kinetics. J Biol Chem 272: 20364-20372.

Innocenti A, Casini A, Alcaro MC, Papini AM, Scozzafava A, Supuran CT (2004). Carbonic anhydrase inhibitors: the first on-resin screening of a 4-sulfamoylphenylthiourea library. Jo Med Chem 47: 5224-5229.

Jiang Y, Su JT, Zhang J, Wei X, Yan YB, Zhou HM (2008). Reshaping the folding energy landscape of human carbonic anhydrase II by a single point genetic mutation Pro237His. Int J Biochem Cell Biol 40: 776-788.

Kockar F, Maresca A, Aydin M, Isik S, Turkoglu S, Sinan S, Arslan O, Guler OO, Turan Y, Supuran CT (2010). Mutation of Phe91 to Asn in human carbonic anhydrase I unexpectedly enhanced both catalytic activity and affinity for sulfonamide inhibitors. Bioorgan Med Chem 18: 5498-5503.

Krebs JF, Fierke CA (1993). Determinants of catalytic activity and stability of carbonic anhydrase-II as revealed by random mutagenesis. J Biol Chem 268: 948-954.

Krebs JF, Rana F, Dluhy RA, Fierke CA (1993). Kinetic and spectroscopic studies of hydrophilic amino acid substitutions in the hydrophobic pocket of human carbonic anhydrase II. Biochemistry 32: 4496-4505.

Mete E, Comez B, Inci Gul H, Gulcin I, Supuran CT (2016). Synthesis and carbonic anhydrase inhibitory activities of new thienyl-substituted pyrazoline benzenesulfonamides. J Enzyme Inhib Med Chem 31: 1-5.

Mikulski R, Avvaru BS, Tu C, Case N, McKenna R, Silverman DN (2011a). Kinetic and crystallographic studies of the role of tyrosine 7 in the active site of human carbonic anhydrase II. Arch Biochem Biophys 506: 181-187.

Mikulski R, Domsic JF, Ling G, Tu CK, Robbins AH, Silverman DN, McKenna R (2011b). Structure and catalysis by carbonic anhydrase II: role of active-site tryptophan 5. Arch Biochem Biophys 516: 97-102.

Nair SK, Calderone TL, Christianson DW, Fierke CA (1991). Altering the mouth of a hydrophobic pocket - structure and kinetics of human carbonic anhydrase-II mutants at residue Val-121. J Biol Chem 266: 17320-17325.

Nair SK, Christianson DW (1993). Structural consequences of hydrophilic amino acid substitutions in the hydrophobic pocket of human carbonic anhydrase II. Biochemistry 32: 4506-4514.

Sastry GM, Adzhigirey M, Day T, Annabhimoju R, Sherman W (2013). Protein and ligand preparation: parameters, protocols, and influence on virtual screening enrichments. J Comput Aid Mol Des 27: 221-234.

Scott AD, Phillips C, Alex A, Flocco M, Bent A, Randall A, O'Brien R, Damian L, Jones LH (2009). Thermodynamic optimisation in drug discovery: a case study using carbonic anhydrase inhibitors. ChemMedChem 4: 1985-1989.

Senturk M, Gulcin I, Beydemir S, Kufrevioglu OI, Supuran CT (2011). In vitro inhibition of human carbonic anhydrase I and II isozymes with natural phenolic compounds. Chem Biol Drug Des 77: 494-499.

Silverman DN, Lindskog S (1988). The catalytic mechanism of carbonic-anhydrase - implications of a rate-limiting protolysis of water. Accounts Chem Res 21: 30-36.

Supuran CT (2008). Carbonic anhydrases: novel therapeutic applications for inhibitors and activators. Nat Rev Drug Discov 7: 168-181.

Supuran CT, Scozzafava A (2007). Carbonic anhydrases as targets for medicinal chemistry. Bioorgan Med Chem 15: 4336-4350.

Turkoglu S, Maresca A, Alper M, Kockar F, Isik S, Sinan S, Ozensoy O, Arslan O, Supuran CT (2012). Mutation of active site residues Asn67 to Ile, Gln92 to Val and Leu204 to Ser in human carbonic anhydrase II: influences on the catalytic activity and affinity for inhibitors. Bioorgan Med Chem 20: 2208-2213.

Verpoorte JA, Mehta S, Edsall JT (1967). Esterase activities of human carbonic anhydrases B and C. J Biol Chem 242: 4221-4229.

West D, Kim CU, Tu CK, Robbins AH, Gruner SM, Silverman DN, McKenna R (2012). Structural and kinetic effects on changes in the CO_2 binding pocket of human carbonic anhydrase II. Biochemistry 51: 9156-9163.

Wu MJ, Jiang Y, Yan YB (2011). Impact of the 237th residue on the folding of human carbonic anhydrase II. Int J Mol Sci 12: 2797-2807.

Yaseen R, Ekinci D, Senturk M, Hameed AD, Ovais S, Rathore P, Samim M, Javed K, Supuran CT (2016). Pyridazinone substituted benzenesulfonamides as potent carbonic anhydrase inhibitors. Bioorg Med Chem Lett 26: 1337-1341.

Supplemental Content

Figure S1. SDS-PAGE analysis of purified SUMO fusion human carbonic anhydrase II Lane 1: lysate; Lanes 2–3: elution; Lanes 4–6: unbound-flow through; 7–8: wash; Lane 9: marker.

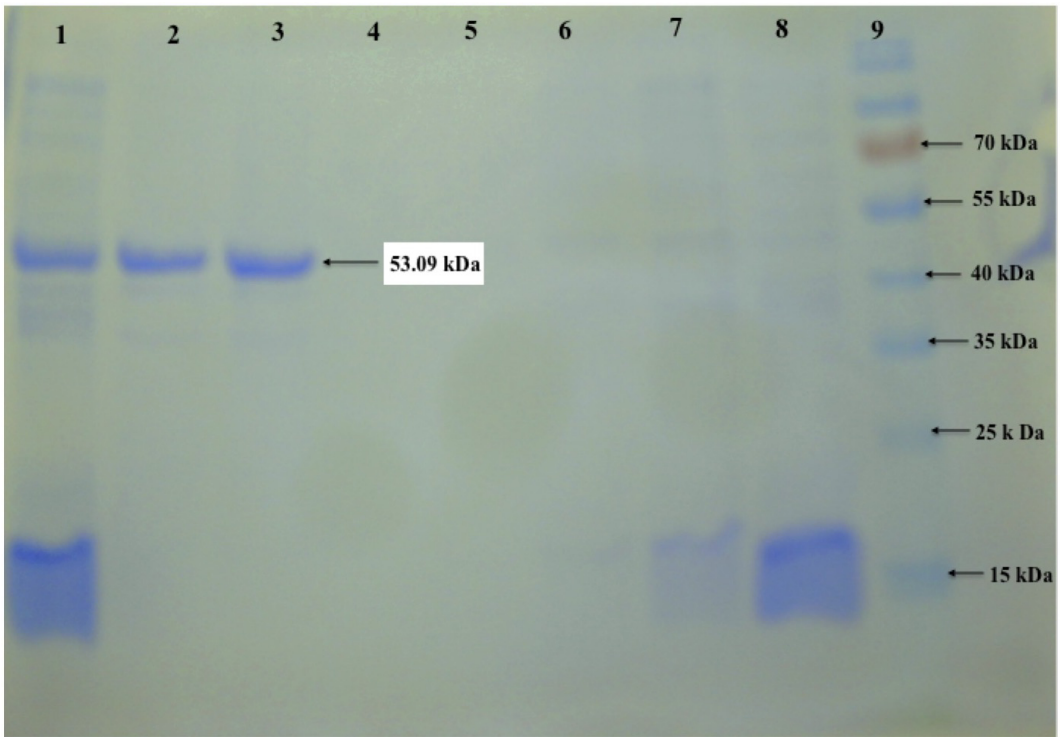

Figure S2. SDS-PAGE analysis of cleavage of the SUMO-hCAII fusion protein by SUMO protease. Lane 1: marker; Lane 2: SUMO-hCA II, hCA II, SUMO; Lane 3: SUMO-hCA II.